


Article

Design and Evaluation of ACFC—An Automatic Cloud/Fog Collector

Ping Du ¹, Xiaoling Nie ¹, Hongtao Liu ², Zhiru Hou ², Xiaole Pan ³, Hang Liu ³, Xinghui Liu ¹, Xinfeng Wang ⁴ , Xiaomin Sun ⁴ and Yan Wang ^{1,*}

¹ School of Environmental Science and Engineering, Shandong University, Qingdao 266237, China

² Renhezhihai Intelligent Technology (Shandong) Co., Ltd., Weifang 261000, China

³ Institute of Atmospheric Physics, Chinese Academy of Sciences, Beijing 100029, China

⁴ Environment Research Institute, Shandong University, Qingdao 266237, China

* Correspondence: wy@sdu.edu.cn

Abstract: Cloud and fog droplets are essential in atmospheric chemistry since they affect the distribution and chemical transformation of pollutants. Collecting sufficient volumes using cloud/fog samplers is the premise of cloud fog chemical studies. Accurate identification of fog events and high collection efficiency are the basic principles of sampler design. Therefore, an automatic cloud/fog collector (ACFC) has been designed, fabricated, and extensively tested for collecting samples of cloud/fog water. The control box and standard sensors for air temperature, relative humidity, and instantaneous rainfall were used to ensure sampling automation. Airflow measurement was used to guarantee the stability of the airspeed on the inlet section, and the airspeed is 7.5 m s^{-1} . Moreover, the median collection rate of ACFC was $160\text{--}220 \text{ mL h}^{-1}$, which was tested via a simulation experiment. To evaluate the actual performance of the device in the field, we obtained eight samples of cloud fog water from Shanghuang Observatory in eastern China from the summer through the fall of 2022. Collection rates varied from 62 to 169 mL h^{-1} . For a cloud/fog sampler equipped with multiple sensors, the ACFC has excellent sampling efficiency in thick fog, sufficient cloud fog water samples can be collected in weak fog, and it can precisely identify fog mingled with rain.

Keywords: cloud fog water; sampler; multiple sensors; collection efficiency



Citation: Du, P.; Nie, X.; Liu, H.; Hou, Z.; Pan, X.; Liu, H.; Liu, X.; Wang, X.; Sun, X.; Wang, Y. Design and Evaluation of ACFC—An Automatic Cloud/Fog Collector. *Atmosphere* **2023**, *14*, 563. <https://doi.org/10.3390/atmos14030563>

Received: 30 December 2022

Revised: 14 March 2023

Accepted: 14 March 2023

Published: 16 March 2023



Copyright: © 2023 by the authors. Licensee MDPI, Basel, Switzerland. This article is an open access article distributed under the terms and conditions of the Creative Commons Attribution (CC BY) license (<https://creativecommons.org/licenses/by/4.0/>).

1. Introduction

Cloud and fog play a key role in atmospheric chemistry by affecting the distribution and chemical transformation of aerosols and trace gases. They promote the formation of acid rain and exert a far-reaching influence on the generation of secondary aerosols, haze pollution, and the air microbial community [1–4]. Collecting sufficient amounts of cloud fog water to avoid rain interference for cloud/fog water chemical analysis is an important problem in fog research at remote sites, primarily distributed in inland river basins, coastal cities, plateaus, and mountain areas.

The ideal cloud/fog water harvesting device should recover most of the liquid phase quickly while allowing the gas phase to pass freely. However, larger water drops resulting from wind-driven rainfall and drizzles are hardly separated from cloud/fog water droplets and can be indistinguishable from the water obtained solely from cloud/fog [5]. Moreover, the cut-off diameter, which is the droplet size threshold below which more than 50% of the droplets are not captured by the sampler, depends on the ambient wind across the strands of the samplers. The chemical composition of cloud/fog water has a strong size-dependent feature [6]. Thus, a sampler equipped with a power unit such as a fan or pump is essential for collecting cloud/fog water for chemical analysis.

More than 30 types of samplers [7] have been developed and applied to the study of cloud fog chemistry. These samplers are mainly divided into passive cloud fog samplers and active cloud fog samplers. Passive cloud fog samplers [8–10] are commonly used to provide

domestic water in regions with less precipitation [11]. They are also sometimes used to collect cloud/fog water for chemical analysis during long-term monitoring and have complete auxiliary facilities for sample storage. In contrast, active cloud/fog water samplers, such as the Caltech active-strand fog water collector (CASCC) [12], have become the preferred sampling instrument in many studies [13–16]. However, these samplers often encounter problems with rainfall pollution and night fog event identification during practical application. Generally, cloud fog water collection is effective when the relative humidity (RH) is >90%, which is determined using visibility sensors [17], optical rain sensors combined with passive cloud fog samplers [18], or liquid water content (LWC) >10 mg m⁻³ [19–21] to indicate the presence of fog. The drawback is that it is difficult for these samplers to avoid rain pollution and meet the deployment without shelter.

The objective of this study was to develop an automatic cloud/fog collector, named ACFC, with a monitoring system that can accurately identify fog and avoid interference from rainy days. Hence, we introduced a new instantaneous rainfall-monitoring piezoelectric sensor, which is not limited to installation conditions and weak light at night. Furthermore, all sensors were concentrated on a bar, and the bar was mounted on a platform held in place by a tripod. Each of these units can be replaced separately in the field. To evaluate this device, the sampler was tested at a mountainous site and an enclosed laboratory room filled with fog produced by a humidifier. The collection volume, duration, RH, LWC, and other physical parameters of fog droplets were recorded using a clock, measuring cylinder, anemometer, and fog monitor to obtain the collection efficiency related to the proportion of water in the fog.

2. Methods

2.1. Units and Operation of the Sampler

The ACFC can be divided into three units: the sampler, the sensor module, and the programmable logic controller (PLC) control box (Figure 1). The sensor module is integrated into a 600 mm horizontal bar, which can identify fog events and avoid mistaking rain for fog.



Figure 1. Complete view of the ACFC. Above the PLC control box with a platform anchored by a tripod and the sampler with automatic baffle, plus the sensor module.

The sampler comprises two main components: (1) a power unit with a fan and a gradual round hole-shaped element to prevent internal turbulence, and (2) a cloud fog water collection unit with strands and an injection door at the front. The power unit is made of an aluminum alloy, and each part is permanently fixed together and cannot be disassembled in the field. For the shell of the cloud fog water collection unit, we designed a special double-layer structure: the outer layer is made of aluminum alloy, the inner layer

is made of nylon, and the spacing between the two layers is approximately 8 mm. The strands of the cloud fog collection unit are made of Teflon and can be easily removed. The power unit and cloud fog water collection unit can be assembled without screws only after the fog tube is aligned and rotated at a small angle.

The door is attached to a magnet and opens when it is electrified. Cloud fog was drawn by a fan and then passed through six rows of 0.5 mm diameter Teflon strands with a spacing of 1.8 mm [22]. The PLC control box contains PLC; a digital display screen, which can record real-time data (such as sampling time, temperature, humidity, and rainfall); a touch screen and remote control; and electronic components.

The general fog identification signal is typically visible or humid. Peter et al. [23] used a combination of an optical rain sensor and a standard passive fog sampler as the excitation signal at the beginning of fog sampling. After the excitation signal was sent to the sampler, it was turned on when the RH was greater than 90%. Carrillo et al. [17] used a cloud fog detector to detect fog visibility. In this study, automatic sampling is controlled by humidity and instantaneous rainfall, and a temperature sensor is used to prevent icing to protect the instrument. The ACFC is not triggered at temperatures below 0 degrees Celsius. The sampler is turned on when the RH is more than 90% and the instantaneous rainfall is less than 0.1 mm min^{-1} , and it is turned off when the RH is less than 90% or the instantaneous rainfall is more than 0.1 mm min^{-1} .

Air temperature and relative humidity were measured using a PH-M10YT louvered box temperature and humidity sensor. Whether it was raining was detected with a rainfall sensor, and instantaneous rainfall was measured with a PH-1X-001 piezoelectric rain sensor (Wuhan New Puhui Technology Co., Ltd., Wuhan, China). Sampler control and data storage were performed using a B10S-G digital display screen (Xiamen Haiwei Technology Co., Ltd., Xiamen, China) and S7-200 SMART (Siemens (Beijing, China) Co., Ltd.).

2.2. Dimensions and Geometry of the Device

The sampler adopts a double-layer cylindrical barrel structure that satisfies the cleanliness requirements of the cloud fog water collection process and the overall robustness of the body, while meeting the electrical safety requirements of the electric control mechanism circuit layout. Additionally, an acute angle of $30\text{--}40^\circ$ from the vertical direction is optimal for efficient collection when positioning the collection rope net [24].

The target cloud fog water volume collected per event was set to $\geq 50 \text{ mL}$, which is the basic requirement for all chemical components and standard conductivity and pH measurements. The challenge is to collect sufficient samples quickly in a weak fog. To achieve this, the flow rate of the sampler was a minimum of $500 \text{ m}^3 \text{ h}^{-1}$. The minimum fan size to meet this flow rate was 20 cm in diameter. Therefore, the internal diameter of the rear mounting part of the sampler was 210 mm. The diameter of the inlet was 160 mm to satisfy the impact wind speed requirements.

2.3. Collecting Strands Parameter Design

Demoz et al. (1996) [12] praised a comprehensive opinion on the theoretical collection efficiency concepts of an active-strand impingement sampler. The particle size range of cloud fog droplets is typically $5\text{--}50 \text{ }\mu\text{m}$. The physical parameters of the strands were designed and calculated using fluid mechanics based on the particle size range. The dimensionless Stokes number, S_t , is given by the ratio of the stopping distance of the water droplets to the obstacle's characteristic length. The single-strand collection efficiency in a fluid is defined as:

$$S_t = \frac{\rho d_p^2 U \cos\theta}{9\mu d_c} \quad (1)$$

where ρ is the droplet density, d_p (μm) is the droplet diameter, U (m s^{-1}) is the airspeed, θ is the inclination angle of the strand banks from the vertical, μ is the air viscosity, and d_c (μm) is the diameter of the strand. In addition, Demoz et al. (1996) used the equation of

Davidson and Friedlander (1978) [25] to calculate the efficiency η_s of the single-row strands to collect cloud fog droplets. It is expressed in terms of the Stokes number as:

$$\eta_s = \frac{S_t^3}{S_t^3 + 0.753S_t^2 + 2.796S_t - 0.202} \quad (2)$$

They provide the theoretical collection efficiency of the multiple-row strands in a collector as:

$$\eta = 1 - (1 - \eta_s \times f_r)^r \quad (3)$$

where f_r is the fractional coverage per row (cross-sectional area of the strands in a row divided by the total cross-sectional area of the collector), and r is the number of rows.

The core design of an efficient cloud fog droplet collection is to strike an optimal balance between two physical processes with opposing requirements. Dense strands pose an obstacle to air, decreasing the inlet flow, while droplets can only be intercepted if they encounter a strand while passing through the collector. Thus, strands that are excessively dense or sparse make the sampler less efficient, and f_r represents the density of the strands. The most common design for a single-row passive cloud fog water collector is an inverted triangular structure with f_r of 35%. The collection efficiency of double-row passive cloud fog water samplers, measured in fractional coverage, ranges from 20% to 30% [26]. However, the strand mesh is staggered, and the structure of the strands presents an air blockage problem. Shi et al. provided a “harp-type” collection strands [27], which effectively solved the blockage problem of the inverted triangle structure and was suitable for droplet impact situations. The airspeed of an active sampler is higher than that of a passive cloud fog water sampler; thus, the lower 25% fractional coverage and the harp-type strands were selected for the sampler.

The theoretical collection efficiency of the ACFC is determined as a function of the airspeed and the number of rows (Figure 2) under certain circumstances of f_r . As shown in Figure 2, it provides sufficient collection efficiency when the row number is more than 6 at the airspeed of 4 m s^{-1} . Furthermore, the sampler is more efficient when airspeed is more than 6 m s^{-1} at the row number of 6, and the airspeed was equivalent to the flow rate. Therefore, an airspeed of 7 m s^{-1} and the number of rows for the sampler was 6. The designed collection rope is wound on a Teflon-coated frame (Figure 3a), and three strands (6 rows) frames are placed obliquely (Figure 3b) in the sampler.

2.4. Performance Test

2.4.1. Airflow Measurement

Airflow measurements were performed using a TESTO-425 hot-wire anemometer (TESTO Instrument International Trade (Shanghai) Co., Ltd., Shanghai, China; with an 820 mm long probe with integrated temperature sensors) in the inlet area (10 cm in front of the strands). For each measuring point, the mean flow velocity was averaged over 20 s using a 2 s measurement interval. These measurements were carried out in a circular sampling matrix with a diameter of 16 cm and were repeated multiple times under laboratory conditions. The accuracy of the instrument was 0.01 m s^{-1} at low speeds, and the measuring range was $0.01\text{--}20 \text{ m s}^{-1}$.

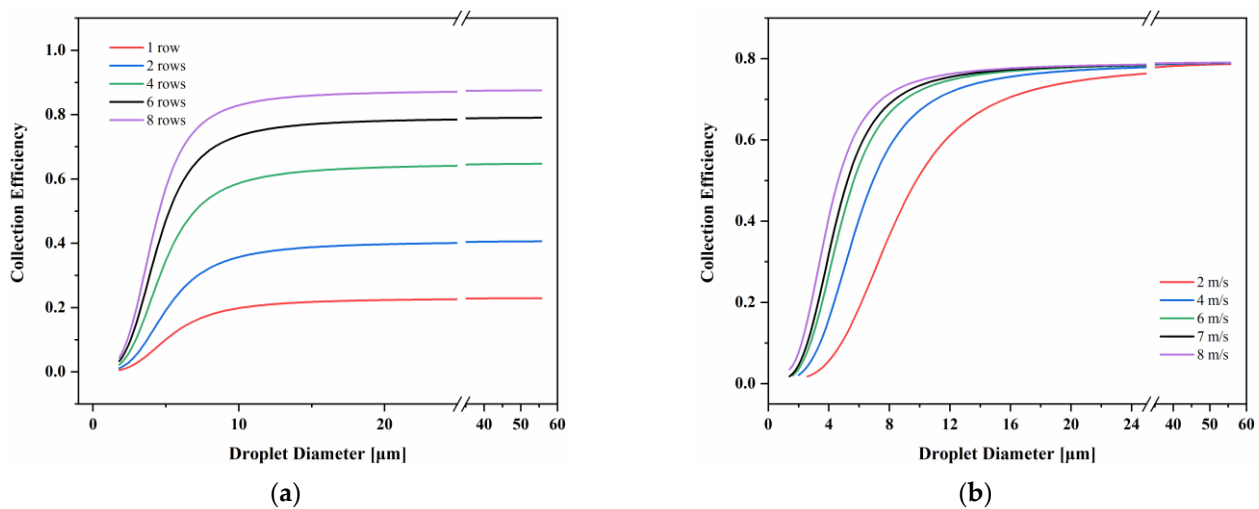


Figure 2. The collection efficiency as a function of droplet diameter at the airspeed of 4 m s^{-1} (a) and the row number of 6 (b).

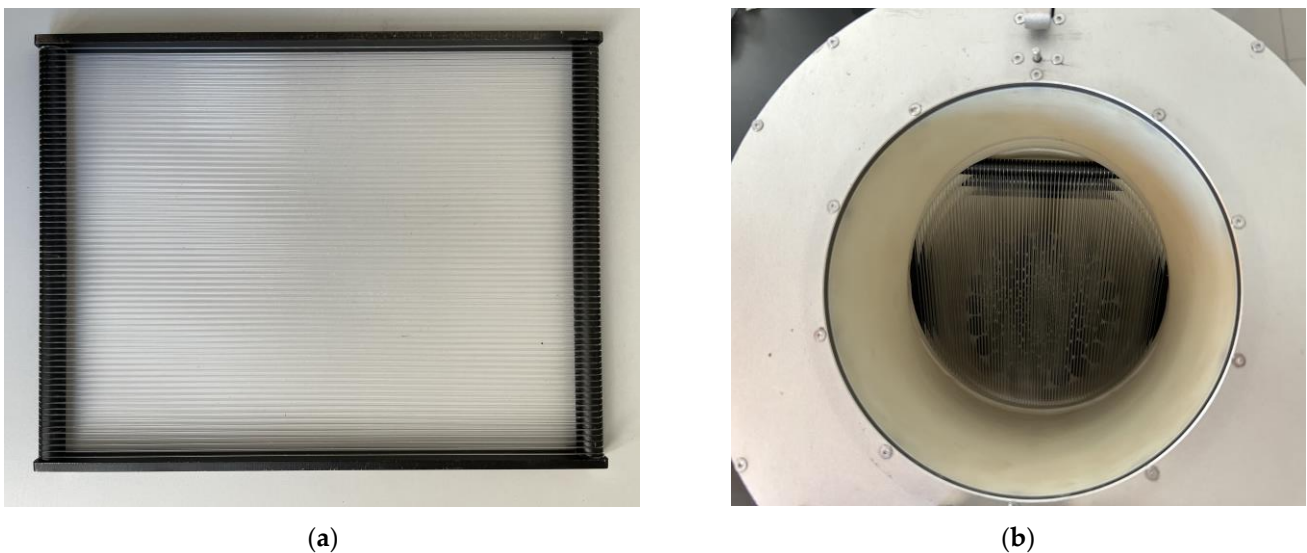


Figure 3. The frame that wraps around the collecting strands (a) and the position of frames in the sampler (b).

2.4.2. Cloud Fog Water Collection Simulation Experiment

To establish the relationship between the LWC and collection rate for the cloud fog sampler, we estimated the influence of the droplet number and diameter on the collection volume. The tests were conducted in a laboratory environment, with the amount of cloud fog controlled by four industrial humidifiers. The ACFC cloud fog water sampler was validated in a cubic laboratory chamber measuring $2.5 \times 2.5 \times 1.75 \text{ m}^3$. Four industrial humidifiers (Oakes Group, Ningbo, China) with a rated fog output of 1200 mL h^{-1} using ultra-pure water were located at the four corners of the chamber to provide fog droplets with a relatively stable water proportion. A fog monitor (Model FM-120, Droplet Measurement Technologies Inc., Longmont, CO, USA) was placed in the center of the chamber at a vertical distance of 1.2 m from the ground to record the LWC, number concentration (Nc), median volume diameter (MVD), and effective diameter (ED) of the artificial fog [28].

The sampler was equipped with an HMT120 temperature and humidity sensor to meet the requirements for relative humidity measurements during the sampling process. However, the RH data were measured using a CEM DT-321S temperature and humidity

sensor with higher sensitivity and accuracy, owing to its high precision. The collection volumes were recorded manually using a measuring cylinder for 30 min. A set of interval values of RH was recorded every 10 min.

2.5. Field Test

The field test of the ACFC sampler was performed at the Shanghuang Observatory of the Chinese Academy of Sciences in eastern China (28.58° N, 119.51° E, 1113 m a.s.l.) from 18 July 2022 to 29 October 2022. A building is located at the top of Damaojian Mountain, which houses the atmospheric boundary layer top ecological environment observation station and ecological environment across the alpine research platform. The station is suitable for cloud monitoring due to its tendency for foggy conditions in summer. Monitoring activities for atmospheric pollutants and greenhouse gases are also carried out synchronously. The test location was on the fourth floor of the building, 15 m above ground. There were no industrial pollution sources in the 50 square kilometers of the site.

3. Results and Discussions

3.1. Inlet Flow Rate

To ensure that the inlet volume satisfied the cloud fog water collection volume requirements, an inlet airspeed test was conducted. An isometric cylinder with a circle of holes spaced 1 cm apart is added in the inlet of the ACFC, and the other holes are blocked when the probe penetrates a small hole, ensuring the airtightness of the airspeed measurements. The hole in the cylinder and the length of the probe protruding into the hole determine the position of the velocity measurement point.

The airspeed on the circular cross-sectional inlet edge was below 4.00 m s^{-1} , which is half the airspeed of the central section. At the measured airspeed, the droplet cut-off diameter was about $4.5 \mu\text{m}$, whereas a drop of airspeed to 4.00 m s^{-1} would increase the cut-off diameter to $6.5 \mu\text{m}$. Significant size fractionation of the droplet spectrum occurred when the airspeed was below 2 m s^{-1} . The measured airspeeds varied with the spatial distribution, in which the airspeed was $7.06\text{--}8.32 \text{ m s}^{-1}$ (Figure 4), which translates to a flow rate of $511\text{--}602 \text{ m}^3 \text{ h}^{-1}$ at full load.

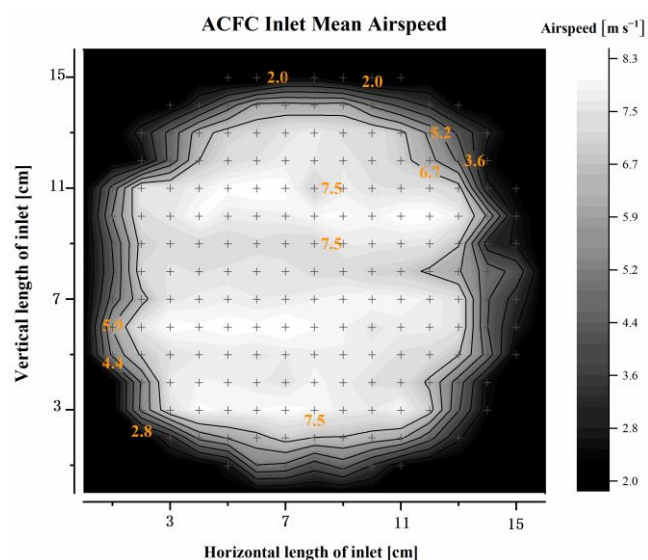


Figure 4. The distribution of airflow velocity measured under laboratory conditions. The panel shows the inlet flow field. Black dots of the cross indicate the points of measurement (mean of 10 values).

3.2. Collection Efficiency

The purpose of this section was to quantitatively evaluate the collection rate of the ACFC. The physical parameters of LWC and visibility characterize the size of the fog. Thus, we need to determine the relationship between collection efficiency and LWC. The

collection rate (Cr) of the sampler is the product of the collection efficiency, intake flow rate, and LWC, which is defined as:

$$Cr = \eta * Q * LWC \quad (4)$$

where η is the collection efficiency, and Q is the inlet flow rate.

To obtain a more accurate assessment of collection efficiency, it is possible to calculate the theoretical droplet distributions and derive the overall collection efficiency for a given LWC value. For the assumption of theoretical droplet distributions, we used $\beta(d_p)$, a parameter representing the number of droplets per unit volume of a droplet over a specific diameter range, using the same approach as Demoz et al. (1996) [24], who used parameterizations presented by Best (1951) [29]. They defined the volume fraction of droplets with diameters between d_p and $d_p + \Delta d_p$ (in μm) as:

$$\beta_{(d_p)} = \left(\frac{n}{a}\right) \left(\frac{d_p}{a}\right)^{n-1} \exp - \left(\frac{d_p}{a}\right)^n \quad (5)$$

where d_p is the droplet diameter, with parameters $n = 3.27$ and $a = (909.1 \cdot LWC)^{0.559}$, and LWC is expressed in g m^{-3} .

As shown in Figure 5a, the peak of typical droplet size distributions moved in the direction of a smaller diameter with the decrease of LWC. Thus, this method has vast uncertainty regarding the droplet diameter distribution with a low LWC. The collection efficiency increased sharply when $LWC < 0.05 \text{ g m}^{-3}$, and increased slowly to 0.8 when $LWC > 0.1 \text{ g m}^{-3}$ (Figure 5b). Furthermore, the relationship between the collection rate and LWC was linear when $LWC > 0.1 \text{ g m}^{-3}$.

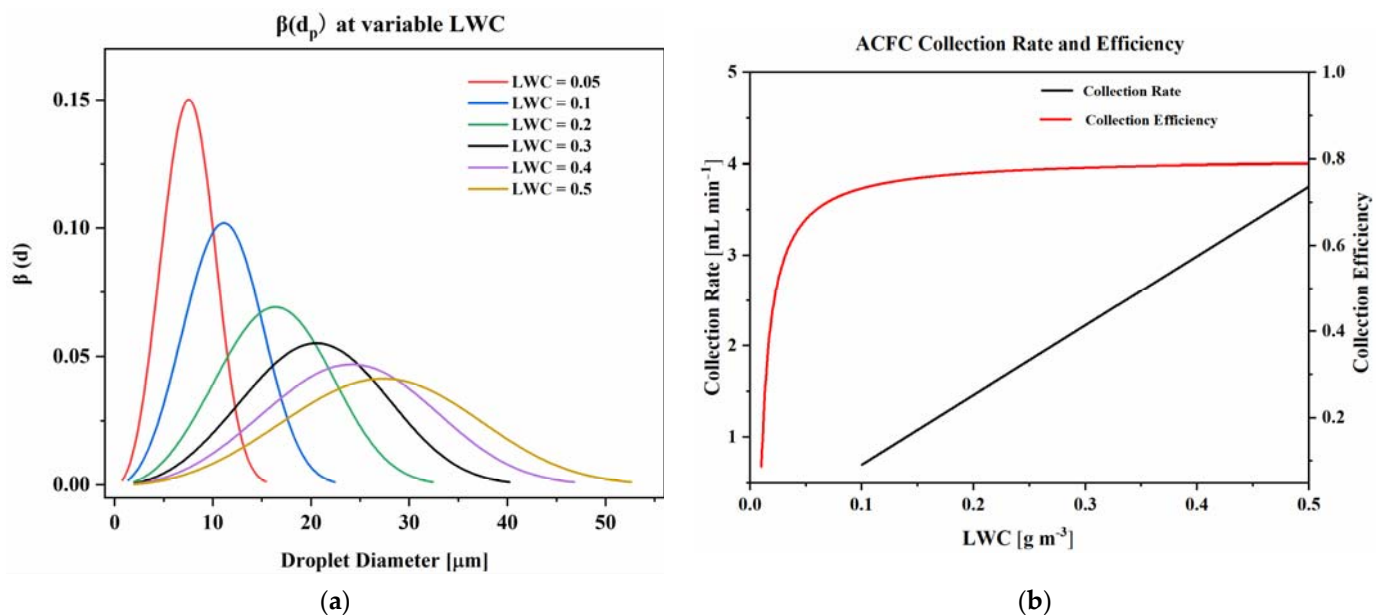


Figure 5. (a) $\beta(d_p)$ as a function of some given LWC values. (b) ACFC collection rate and collection efficiency as a function of liquid water content (LWC). Droplet spectra were calculated with the same approach as in Demoz et al. (1996) using the theoretical droplet size spectra according to Best (1951).

3.3. Sampling Performance in Artificial Fog

To explore the influence of LWC and RH on the collection efficiency, fog collection experiments were conducted in a relatively sealed artificial fog chamber, where the primary monitoring equipment for the microphysical parameters of the fog was FM-120. The FM-120 is a forward scatterer based on the Mie scattering principle that displays fog microphysical parameters in real time. The sampling efficiency of FM-120 depends on two parameters: the sampling angle and the ratio of the ambient wind speed to the sampled wind speed,

both of which can be ignored in a simulated environment. The flow rate of FM-120 was $1 \text{ m}^3 \text{ min}^{-1}$, and the time resolution was 1 s.

The relative humidity fluctuation was maintained within a constant range by adjusting the fog output of the humidifiers using ultra-pure water. The fog collection experiment with a monitoring period of 2 h was carried out, and the collection volume was measured with a cylinder every half hour. The sampling amounts per hour varied with air relative humidity (Figure 6a). When the RH was lower than 94%, the sampling rate was 5 mL h^{-1} . When the RH was between 94% and 98%, the sampling volume could be as high as $160\text{--}220 \text{ mL h}^{-1}$. The sampling rate reached 560 mL h^{-1} when RH was greater than 98%. Thus, the collection volumes at different LWC values monitored by the FM-120 were added to verify the results. The addition shows that the collection rate was 600 mL h^{-1} when the LWC was 0.43 g m^{-3} , which is similar to 560 mL h^{-1} (Figure 6b). The sampling efficiency reaches the maximum value, and it does not increase with the increase in LWC when the LWC is greater than 0.2 g m^{-3} .

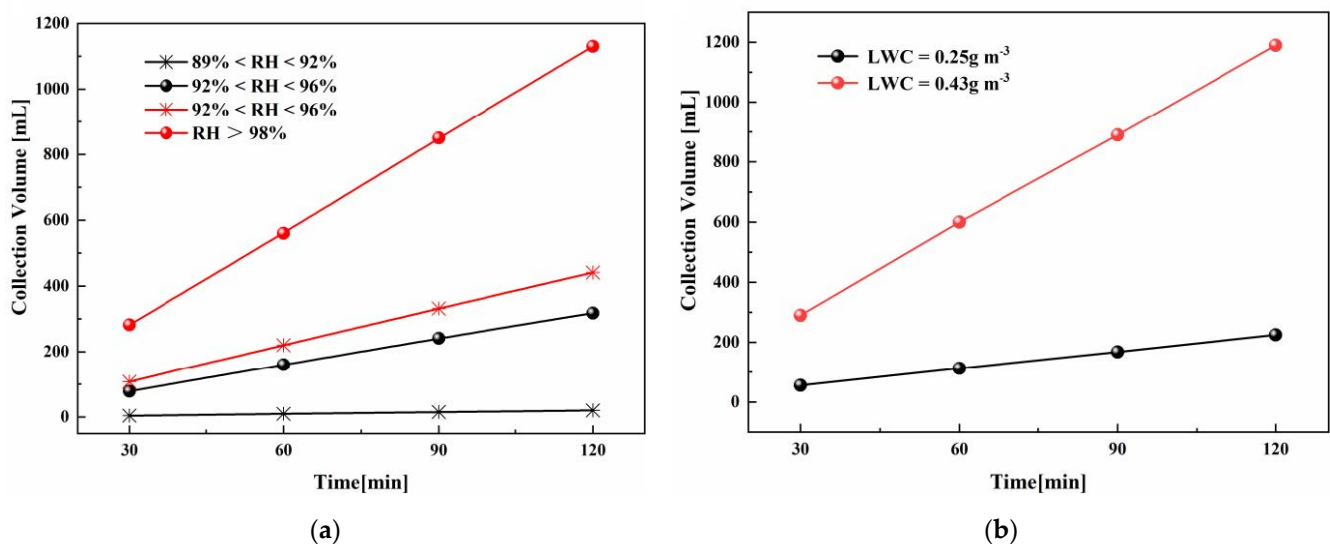


Figure 6. (a) The relationship between collection volume and duration of the sampler in different humidity ranges. (b) The relationship between collection volume and duration of the sampler at $\text{LWC} = 0.25 \text{ g m}^{-3}$ and $\text{LWC} = 0.43 \text{ g m}^{-3}$.

Although the value of LWC is subject to clear monitoring underestimation, the collection rate of 600 mL h^{-1} requires an LWC of 1.5 g m^{-3} based on Equation (4) introduced in Section 3.2. This also indicates that the ACFC has a high collection efficiency in high-moisture-content fog. Due to the limitation of the ultrasonic oscillation frequency of the humidifier, which results in droplet diameters being more than 90% distributed below $5 \mu\text{m}$, the monitoring value of FM-120 on the LWC was underestimated. Therefore, the experiment only conducted the fog droplet sampling experiment under the condition of high LWC levels ($\text{LWC} > 0.2 \text{ g m}^{-3}$) and used FM-120 to conduct real-time monitoring of the physical parameters of the fog droplet.

The parameters of the simulated fog in the two controlled LWC experiments were further analyzed to explore the reasons for the underestimation of LWC. The characteristics of the droplet spectrum showed that the droplet diameters in the two tests were mainly concentrated in the range of $3\text{--}6 \mu\text{m}$, which was less than $14 \mu\text{m}$ (Figure 7). However, the peak mode N_c increased from 900 to 1300 cm^{-3} when LWC changed from 0.25 to 0.43 g m^{-3} . It can be observed that the simulated fog missed the process of small droplets colliding and combining into large droplets in the natural environment. The diameter of the droplets did not increase, but N_c was significantly higher. The peak mode of the number concentration was 45% higher than that of the first fog experiment, indicating that the increase in LWC

in the second fog simulation experiment was related only to the increase in the number of droplets.

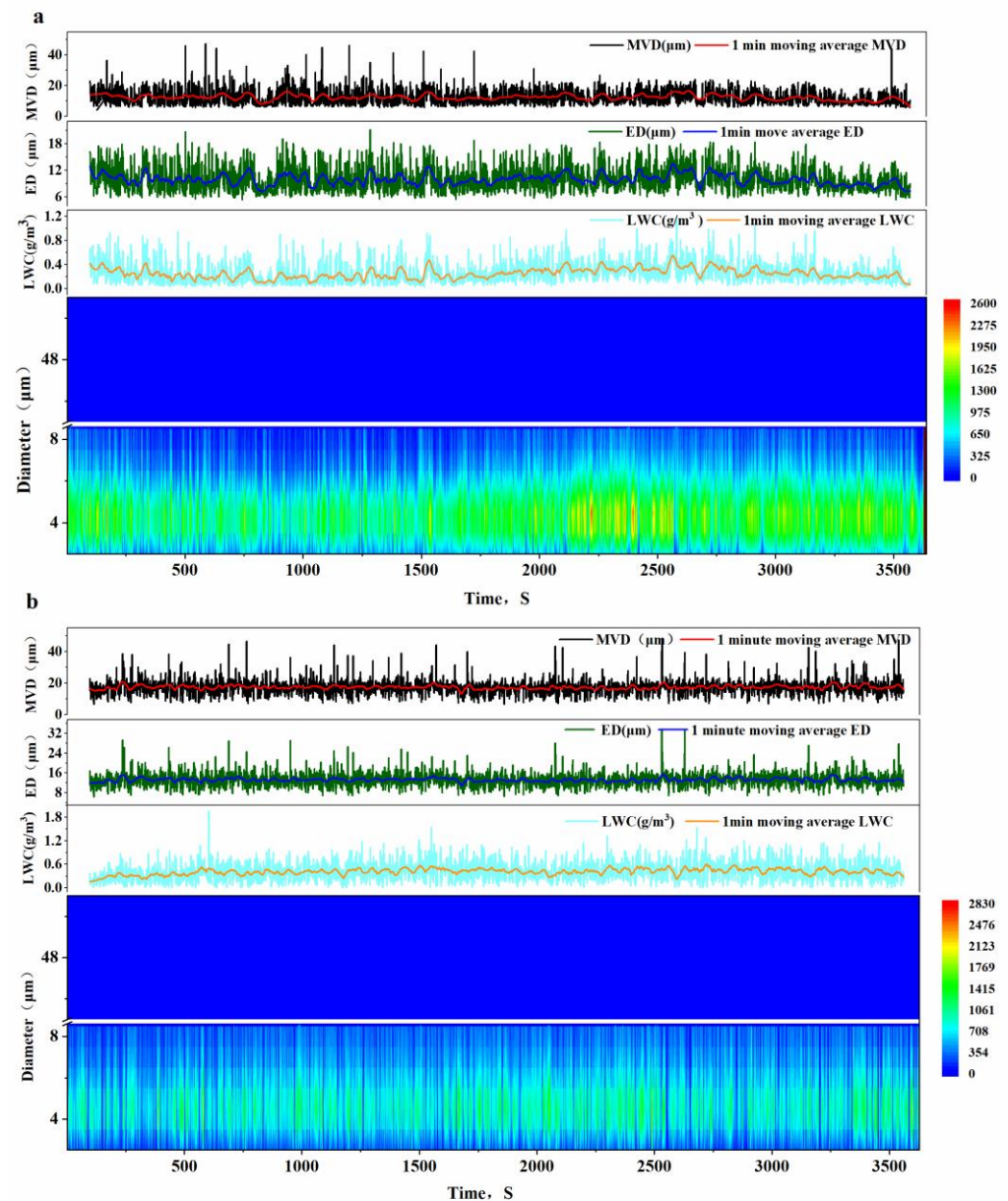


Figure 7. ED, MVD, LWC, and the relationship between N_c with fog droplet diameter at mean LWC of 0.25 g m^{-3} (a) and 0.43 g m^{-3} (b). Effective diameter (ED) represents the mean diameter of droplets, median volume diameter (MVD) represents the median diameter of droplets, and number concentration (N_c) represents the number of droplets in unit volume.

3.4. Collection Performance in the Field

The fog sampling campaign was tested at Atmospheric Boundary Layer Eco-Environmental Shanghuang Observatory during the summertime fog seasons of 2022. The purpose of sampling the fog was to test the collection performance of ACFC in the actual environment. From 17 July to 29 October (103 days), there were 8 cloud fog water samples collected with volumes $>81 \text{ mL}$ (Figure 8). The daily mean collection volume was $286 \pm 137 \text{ mL}$ and only one sample was collected in the daytime, always at night or early morning hours. The PLC control box produced a signal for 10 events, meaning that the ACFC was triggered for these 10 events, but for 2 of these events, no sample was collected. Possible reasons for no sample collected are that the RH is higher than 90%, but the mean LWC of the cloud fog event is lower than 0.05 g m^{-3} .

Furthermore, 9 rainfall events occurred during fog season, and rainwater was not wrongly collected as cloud fog water samples.

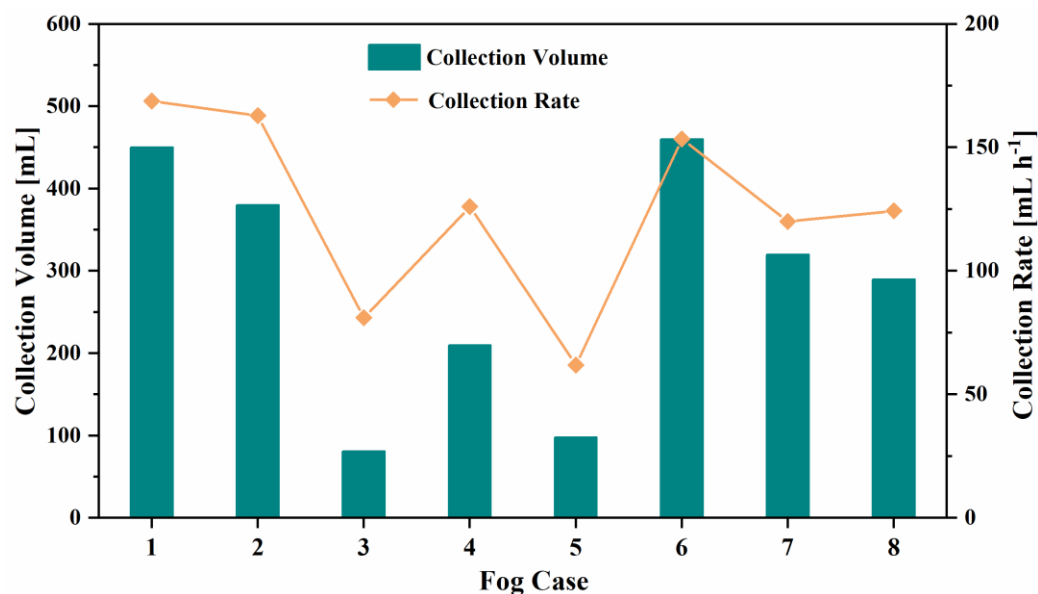


Figure 8. The volumes of eight cloud samples were collected at Shanghuang Observatory from July to October 2022. The collection rates were calculated by collection volumes and durations.

In the summer of 2022 at Shanghuang Observatory, the ACFC was set to trigger on based $RH > 90\%$ and instantaneous rainfall $< 0.1 \text{ mm min}^{-1}$. Eight cloud fog water samples were collected for basic inorganic chemical analysis, of which seven cloud fog events were collected at night, indicating its superiority over low-cost visibility sensors. Most of the dates on which the rain occurred are not the same as the dates on which the cloud fog water samples were collected, and the sampler accurately identified rainy days.

In the eight collected fog events, the LWC ranged from 0.11 to 0.42 g m^{-3} , and the RH is more than 95%. In two mist events ($LWC < 0.2 \text{ g m}^{-3}$), the collection rates of cloud fog water were 61.9 and 81 mL h^{-1} , respectively, which was sufficient to support obtaining the required sample volume of 100 mL . The collection rate was more than 120 mL h^{-1} , and the collection volume was more than 400 mL in thick fog ($RH > 98\%$).

4. Conclusions

The ACFC, an automatic cloud/fog collector, was provided for development and calculation verification and consisted of the sampler itself, the sensor module, and the PLC control box. Collection experiments were conducted in a simulation fog chamber with gradient humidity and an actual environment. The ACFC has an excellent collection efficiency (90%) when the RH is more than 94%, or when the LWC is more than 0.1 g m^{-3} . The collection rates in field tests were slightly lower than that in the simulation experiments; the collection volumes were sufficient for the examination of the basic inorganic chemical composition of the collected cloud fog water. Moreover, instantaneous rainfall sensors, doors, and double structures of the fuselage were added to the device, which jointly ensured the accuracy, cleanliness, and safety of the automatic sampling. The main benefit of ACFC is its ease of use and relatively low cost, in dealing with the complex meteorological conditions in cloud observation. The preliminary sampling scheme can be judged by the basic parameters of cloud fog due to the quantization of the relationship between sampling rate and RH and LWC. The ACFC has excellent collection efficiency and can precisely identify fog mingled with rain. Future studies should emphasize accurate segmentation of the size of cloud fog droplets.

Author Contributions: Conceptualization, Y.W.; Methodology, Y.W. and P.D.; Validation, Y.W. and X.W.; Formal Analysis, P.D. and X.N.; Investigation, P.D., X.L., H.L. (Hang Liu) and X.P.; Resources, Z.H., H.L. (Hongtao Liu), X.P. and P.D.; Data Curation, P.D.; Writing—Original Draft Preparation, P.D.; Writing—Review and Editing, X.N. and X.S.; Visualization, P.D.; Supervision, Y.W., X.N. and X.S.; Project Administration, Y.W., X.S., X.W. and H.L. (Hongtao Liu); Funding Acquisition, Y.W. All authors have read and agreed to the published version of the manuscript.

Funding: This work was financially supported by the National Natural Science Foundation of China (22176112), the Natural Science Foundation of Shandong Province (ZR2021MD028), and the China Postdoctoral Science Foundation (2022M711893).

Institutional Review Board Statement: Not applicable.

Informed Consent Statement: Not applicable.

Data Availability Statement: Not applicable.

Acknowledgments: The authors appreciate Jianmin Chen at Fudan University for guidance during instrument development and experimental design. The authors thank the Atmospheric Boundary Layer Eco-Environmental Shanghuang Observatory, Chinese Academy of Sciences for supplying the experimental site and assisting in collecting cloud water samples.

Conflicts of Interest: The authors declare no conflict of interest.

References

1. Harris, E.; Sinha, B.; Van Pinxteren, D.; Tilgner, A.; Fomba, K.W.; Schneider, J.; Roth, A.; Gnauk, T.; Fahlbusch, B.; Mertes, S. Enhanced role of transition metal ion catalysis during in-cloud oxidation of SO₂. *Science* **2013**, *340*, 727–730. [[CrossRef](#)]
2. Ervens, B. Modeling the processing of aerosol and trace gases in clouds and fogs. *Chem. Rev.* **2015**, *115*, 4157–4198. [[CrossRef](#)] [[PubMed](#)]
3. Wei, M.; Xu, C.; Chen, J.; Zhu, C.; Li, J.; Lv, G. Characteristics of bacterial community in cloud water at Mt Tai: Similarity and disparity under polluted and non-polluted cloud episodes. *Atmos. Chem. Phys.* **2017**, *17*, 5253–5270. [[CrossRef](#)]
4. Zhao, H.; Meng, B.; Sun, G.; Lin, C.-J.; Feng, X.; Sommar, J. Chemistry and Isotope Fractionation of Divalent Mercury during Aqueous Reduction Mediated by Selected Oxygenated Organic Ligands. *Environ. Sci. Technol.* **2021**, *55*, 13376–13386. [[CrossRef](#)] [[PubMed](#)]
5. Frumau, K.A.; Burkard, R.; Schmid, S.; Bruijnzeel, L.; Tobón, C.; Calvo-Alvarado, J.C. A comparison of the performance of three types of passive fog gauges under conditions of wind-driven fog and precipitation. *Hydrol. Process.* **2011**, *25*, 374–383. [[CrossRef](#)]
6. Moore, K.F.; Sherman, D.E.; Reilly, J.E.; Collett, J.L. Drop size-dependent chemical composition in clouds and fogs. Part I. Observations. *Atmos. Environ.* **2004**, *38*, 1389–1402. [[CrossRef](#)]
7. Roman, P.; Polkowska, Z.; Namieśnik, J. Sampling procedures in studies of cloud water composition: A review. *Crit. Rev. Environ. Sci. Technol.* **2013**, *43*, 1517–1555. [[CrossRef](#)]
8. Daube Jr, B.; Kimball, K.D.; Lamar, P.A.; Weathers, K.C. Two new ground-level cloud water sampler designs which reduce rain contamination. *Atmos. Environ.* **1987**, *21*, 893–900. [[CrossRef](#)]
9. Krämer, M.; Schütz, L. On the collection efficiency of a rotating arm collector and its applicability to cloud-and fogwater sampling. *J. Aerosol. Sci.* **1994**, *25*, 137–148. [[CrossRef](#)]
10. Lange, C.A.; Matschullat, J.; Zimmermann, F.; Sterzik, G.; Wienhaus, O. Fog frequency and chemical composition of fog water—A relevant contribution to atmospheric deposition in the eastern Erzgebirge, Germany. *Atmos. Environ.* **2003**, *37*, 3731–3739. [[CrossRef](#)]
11. Schemenauer, R.S.; Cereceda, P. The quality of fog water collected for domestic and agricultural use in Chile. *J. Appl. Meteorol. Clim.* **1992**, *31*, 275–290. [[CrossRef](#)]
12. Daube, B.C., Jr.; Flagan, R.C.; Hoffmann, M.R. Active Cloudwater Collector. U.S. Patent No. 4,697,462, 6 October 1987.
13. Michna, P.; Schenk, J.; Werner, R.A.; Eugster, W. MiniCASCC—A battery driven fog collector for ecosystem research. *Atmos. Res.* **2013**, *128*, 24–34. [[CrossRef](#)]
14. Wang, W.; Xu, W.; Collett Jr, J.L.; Liu, D.; Zheng, A.; Dore, A.J.; Liu, X. Chemical compositions of fog and precipitation at Sejila Mountain in the southeast Tibetan Plateau, China. *Environ. Pollut.* **2019**, *253*, 560–568. [[CrossRef](#)]
15. Sun, L.; Wang, Y.; Yue, T.; Yang, X.; Xue, L.; Wang, W. Evaluation of the behavior of clouds in a region of severe acid rain pollution in southern China: Species, complexes, and variations. *Environ. Sci. Pollut. R.* **2015**, *22*, 14280–14290. [[CrossRef](#)]
16. Lu, C.; Niu, S.; Tang, L.; Lv, J.; Zhao, L.; Zhu, B. Chemical composition of fog water in Nanjing area of China and its related fog microphysics. *Atmos. Res.* **2010**, *97*, 47–69. [[CrossRef](#)]
17. Carrillo, J.H.; Emert, S.E.; Sherman, D.E.; Herckes, P.; Collett, J.L., Jr. An economical optical cloud/fog detector. *Atmos. Res.* **2008**, *87*, 259–267. [[CrossRef](#)]

18. Zinke, J.; Salter, M.E.; Leck, C.; Lawler, M.J.; Porter, G.C.; Adams, M.P.; Brooks, I.M.; Murray, B.J.; Zieger, P. The development of a miniaturised balloon-borne cloud water sampler and its first deployment in the high Arctic. *Tellus B Chem. Phys. Meteorol.* **2021**, *73*, 1915614. [[CrossRef](#)]
19. Allan, J.D.; Baumgardner, D.; Raga, G.B.; Mayol-Bracero, O.L.; Morales-García, F.; García-García, F.; Montero-Martínez, G.; Borrmann, S.; Schneider, J.; Mertes, S. Clouds and aerosols in Puerto Rico—a new evaluation. *Atmos. Chem. Phys.* **2008**, *8*, 1293–1309. [[CrossRef](#)]
20. Zhang, Q.; Quan, J.; Tie, X.; Huang, M.; Ma, X. Impact of aerosol particles on cloud formation: Aircraft measurements in China. *Atmos. Environ.* **2011**, *45*, 665–672. [[CrossRef](#)]
21. Gultepe, I.; Isaac, G. Aircraft observations of cloud droplet number concentration: Implications for climate studies. *Q. J. Roy. Meteor. Soc.* **2004**, *130*, 2377–2390. [[CrossRef](#)]
22. Weiss-Penzias, P.; Fernandez, D.; Moranville, R.; Saltikov, C. A low cost system for detecting fog events and triggering an active fog water collector. *Aerosol. Air Qual. Res.* **2018**, *18*, 214–233. [[CrossRef](#)]
23. Schemenauer, R.S.; Cereceda, P.; Osses, P. *FogQuest: Fog Water Collection Manual; FogQuest: Sustainable Water Solutions*: Toronto, ON, Canada, 2005.
24. Demoz, B.; Collett, J., Jr.; Daube, B., Jr. On the Caltech active strand cloudwater collectors. *Atmos. Res.* **1996**, *41*, 47–62. [[CrossRef](#)]
25. Davidson, C.; Friedlander, S. A filtration model for aerosol dry deposition: Application to trace metal deposition from the atmosphere. *J. Geophys. Res.-Oceans.* **1978**, *83*, 2343–2352. [[CrossRef](#)]
26. Amato, P.; Ménager, M.; Sancelme, M.; Laj, P.; Mailhot, G.; Delort, A.-M. Microbial population in cloud water at the Puy de Dôme: Implications for the chemistry of clouds. *Atmos. Environ.* **2005**, *39*, 4143–4153. [[CrossRef](#)]
27. Shi, W.; Anderson, M.J.; Tulkoff, J.B.; Kennedy, B.S.; Boreyko, J.B. Fog harvesting with harps. *ACS Appl. Mater. Interfaces* **2018**, *10*, 11979–11986. [[CrossRef](#)]
28. Rangno, A.L.; Hobbs, P.V. Microstructures and precipitation development in cumulus and small cumulonimbus clouds over the warm pool of the tropical Pacific Ocean. *Q. J. Roy. Meteor. Soc.* **2005**, *131*, 639–673. [[CrossRef](#)]
29. Best, A. Drop-size distribution in cloud and fog. *Q. J. Roy. Meteor. Soc.* **1951**, *77*, 418–426. [[CrossRef](#)]

Disclaimer/Publisher’s Note: The statements, opinions and data contained in all publications are solely those of the individual author(s) and contributor(s) and not of MDPI and/or the editor(s). MDPI and/or the editor(s) disclaim responsibility for any injury to people or property resulting from any ideas, methods, instructions or products referred to in the content.